SMJ Saratov Medical Journal

ISSN 2712-8253, Saratov Medical Journal

2026. Volume 7. Issue 1. Article CID e0303
DOI: 10.15275/sarmj.2026.0303

Original article

Reprint

Morphometric model of repair following autologous neurosensory retinal transplantation for giant idiopathic macular holes

Anastasia I. Stepanenko ✉, Rinat R. Fayzrakhmanov, Karina I. Konovalova, Vera N. Borodkina
✉ anasatasiae@yandex.ru

Pirogov National Medical and Surgical Center, Moscow, Russia

Received 13 July 2026, Accepted 29 August 2026

© This article is an open access publication. Russian text published in the *Saratov Journal of Medical Scientific Research,* 2026; 22(3): 305-311. https://doi.org/10.15275/ssmj2203305. ISSN 1995-0039.

Abstract:
Objective: To develop a morphometric model of the structural integration of an autologous neurosensory retinal graft for giant idiopathic macular holes, based on optical coherence tomography (OCT) data.
Materials and methods: This prospective comparative study included 127 patients (127 eyes). Three study groups were designated: edge-to-edge autologous retinal transplantation (n=33), preretinal overlay grafting (n=31), and repair using a free internal limiting membrane (ILM) flap (n=63). OCT was performed preoperatively and at 1, 3, 6, and 12 months postoperatively. The following parameters were evaluated: the macular hole edge elevation index (HEI); retinal thickness outside the edematous zone (known as mean reference thickness over edema [MRTOE]), flap contraction index (FCI), and flap site contraction index (FSCI).
Results: Three distinct phases were identified: early adaptation, structural integration, and morphological remodeling. At 12 months, the HEI of the temporal edge (HEI-t) decreased from 378.10±15.47 to 230.03±5.82 μm in Group 1, from 373.13±15.69 to 343.29±12.02 μm in Group 2, and from 373.96±15.08 to 296.5±14.6 μm in Group 3. For the MRTOE of the temporal edge (MRTOE-t), we observed a statistically significant group-by-time interaction (p<0.001). At 12 months, the FCI values were 1,463.55±183.52 μm and 1,524.45±132.91 μm, while FSCI values were 1,144.64±202.96 μm and 1,196.45±138.22 μm in Group 1 in Group 2, respectively.
Conclusion: The developed morphometric model allows for the quantitative characterization of the successive phases of postoperative repair and the structural integration of an autograft.

Keywords: macular hole, vitreoretinal surgery, autologous retinal transplantation, optical coherence tomography.

Cite as: Stepanenko AI, Fayzrakhmanov RR, Konovalova KI, Borodkina VN. Morphometric model of repair following autologous neurosensory retinal transplantation for giant idiopathic macular holes. *Saratov Medical Journal* 2026; 7(3): e0303. https://doi.org/10.15275/sarmj.2022.0101

Introduction

Despite substantial progress in vitreoretinal surgery, the treatment of giant idiopathic macular holes (IMHs) remains one of the most challenging issues in contemporary ophthalmology. With an increase of the IMH size, the likelihood of achieving optimal anatomical and functional outcomes declines, which limits the efficacy of conventional surgical techniques [1, 2]. As a result, autologous neurosensory retinal transplantation (ART) is employed more and more in recent years, enabling the successful closure of macular defects even in cases of giant IMHs [3, 4].

Most published studies focused on assessing the anatomical closure rate of the IMH and the dynamics of best corrected visual acuity (BCVA) [5]. However, the processes of structural adaptation and integration of the autograft, along with the patterns of retinal remodeling during the postoperative period, remain insufficiently studied [6]. This hinders the objective assessment of the efficacy of various surgical techniques and the prognosis of treatment outcomes [7].

Current optical coherence tomography (OCT) allows for detailed visualization of the retinal microstructure and quantitative assessment of postoperative changes. Yet existing morphometric parameters mainly characterize isolated anatomical features of the macular region, while failing to reflect the complex repair process after ART [8, 9].

That is why, it is highly relevant to develop a morphometric model of repair based on a comprehensive assessment of structural changes in both the transplantation site and the donor zone. This approach will allow us to objectify the processes of postoperative tissue remodeling and evaluate the patterns of structural integration of the autograft.

The *objective* of our study was to develop a morphometric model of the structural integration of an autologous neurosensory retinal graft in cases of giant IMHs, based on OCT data.

Materials and methods

This prospective comparative study included 127 patients (127 eyes) with giant IMHs who underwent surgical

© Stepanenko A.I., Fayzrakhmanov R.R., Konovalova K.I., Borodkina V.N., 2026

treatment between 2025 and 2026. Based on the surgical technique employed, the patients were distributed among three groups. Group 1 consisted of 33 patients who underwent edge-to-edge ART; Group 2 included 31 patients who underwent preretinal overlay grafting; and Group 3 comprised 63 patients who underwent IMH repair using a free internal limiting membrane (ILM) flap (*Table* 1).

All patients underwent a standard ophthalmological examination, which included assessment of BCVA, biomicroscopy, ophthalmoscopy, tonometry, and OCT of the macular region. The examination was performed prior to surgical treatment, as well as at 1, 3, 6, and 12 months postoperatively (*Figure* 1).

To assess the processes of postoperative repair, we performed a sequential analysis of the morphometric parameters in the macular region based on OCT data. We examined HEI, MRTOE, and REA, as well as newly developed quantitative metrics: the flap contraction index (FCI) and the flap site contraction index (FSCI).

Table 1. Preoperative parameter values in the study groups

Parameter	Group	Before treatment	*p*
NMHW	1	976.85±103.22; 962 [918; 998]	0.883
	2	998.42±109.22; 955 [921; 1024]	
	3	984.87±85.7; 946 [912; 1047]	
LMHS	1	1,694.85±167.78; 1,682 [1638; 1739]	0.605
	2	1,669.45±120.85; 1,672 [1593; 1750]	
	3	1,661.14±166.21; 1,628 [1572; 1715]	
VND-t	1	193.82±10.63; 196 [187; 202]	p<0.001 p_{12}=0.001 p_{13}=0.0 p_{23}=0.943
	2	181.39±11.9; 183 [173; 191]	
	3	180.44±13.71; 181 [167; 194]	
VND-n	1	164.06±17.81; 160 [152; 172]	p<0.001 p_{12}=0.001 p_{13}=0.61 p_{23}=0.003
	2	176.87±10.14; 177 [169; 181]	
	3	166.87±11.47; 166 [159; 171]	
RND-t	1	184.27±8.87; 188 [176; 192]	p<0.001 p_{12}=0.005 p_{13}=0.0 p_{23}=0.668
	2	191.74±9.93; 190 [184; 200]	
	3	193.51±8.48; 193 [186; 201]	
RND-n	1	217.37±12.24; 218 [212; 228]	0.286
	2	212.59±13.07; 210 [204; 223]	
	3	213.4±14.07; 215 [201; 224]	
HEI-t	1	378.1±15.47; 381 [372; 390]	0.356
	2	373.13±15.69; 373 [363; 381]	
	3	373.96±15.08; 374 [362; 384]	
HEI-n	1	381.42±17.6; 379 [369; 389]	0.164
	2	387.29±12.26; 385 [380; 399]	
	3	380.27±18.54; 380 [366; 392]	
REA	1	3,538.85±789.18; 3,447 [2746; 4276]	0.446
	2	3,770.55±811.63; 3,814 [3036; 4405]	
	3	3,609.27±695.85; 3,604 [3012; 4273]	
MRTOE-t	1	261±7.54; 261 [255; 266]	p=0.002 p_{12}=0.25 p_{13}=0.002 p_{23}=0.258
	2	264.13±7.2; 263 [258; 270]	
	3	266.85±7.57; 268 [260; 273]	
MRTOE-n	1	262.31±7.52; 262 [257; 269]	0.721
	2	260.88±7.34; 260 [255; 267]	
	3	261.26±7.54; 260 [255; 269]	
BCVA	1	0.07±0.04; 0.05 [0.05; 0.1]	0.379
	2	0.07±0.04; 0.05 [0.05; 0.1]	
	3	0.08±0.05; 0.05 [0.05; 0.1]	

Here and in Figure 1: LMHS, the largest macular hole span; NMHW, the narrowest macular hole width; REA, retinal edema area; HEI, macular hole edge elevation index; MRTOE, mean retinal thickness over edema; RND, RPE-NMHW distance (distance from the retinal pigment epithelium to the NMHW); VND, vitreous-NMHW distance (distance from the vitreous chamber to the NMHW). The suffixes '-t' and '-n' denote the temporal and nasal edges (regions), respectively. Throughout the remainder of this text and in Tables 2-4, quantitative data are presented as the mean ± standard deviation (*M±SD*), as well as the median and interquartile range (*Me* [*Q1*; *Q3*]), to provide a comprehensive characterization of central tendency and variability, including distribution metrics that are robust to outliers.

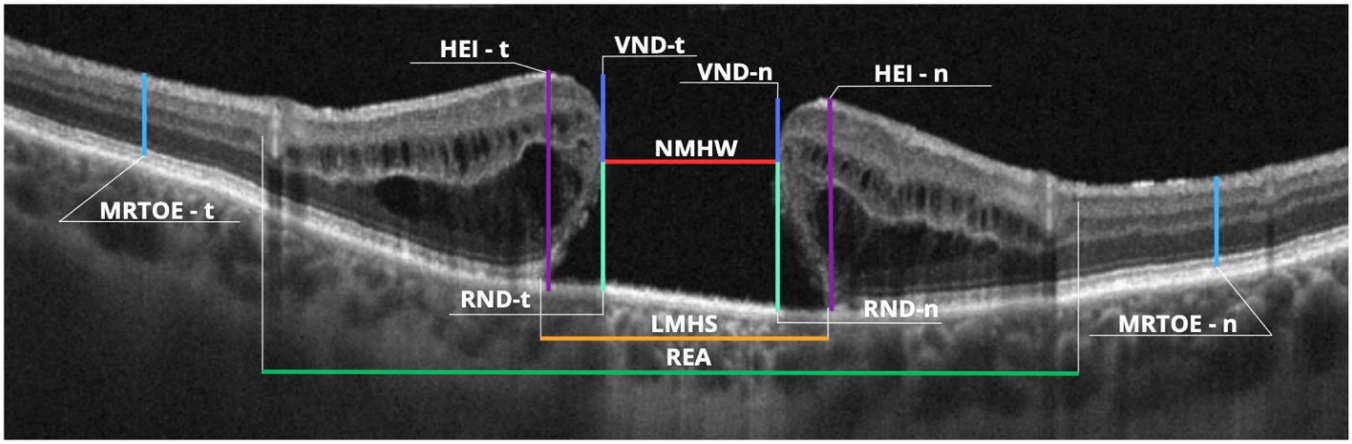

Figure 1. Preoperative ocular computed tomography.

Based on a comprehensive assessment of the dynamics of these morphometric parameters, we developed a morphometric model of repair after ART, reflecting the successive phases of structural adaptation, graft integration, and remodeling of the donor site.

Statistical analysis of the data was conducted using IBM SPSS Statistics 27 (IBM Corp., USA). Quantitative data were presented using both parametric and nonparametric descriptive statistics – specifically, the mean and standard deviation (*M*±*SD*), as well as the median and interquartile range (*Me* [*Q1*; *Q3*]), which allowed for the representation of both central tendencies and variability, as well as the distribution of values, independent of the effect of outliers. Differences among the three study groups were assessed using analysis of variance (ANOVA). In cases where statistically significant intergroup differences were identified, we performed post-hoc pairwise comparisons using the Scheffé's method. The dynamics of the parameters under study during the postoperative period was evaluated using repeated-measures ANOVA (general linear model), assessing the factors of *time* and *group*, as well as the *time* × *group* interaction. Differences were considered statistically significant at $p<0.05$.

Results

An analysis of the HEI dynamics revealed differences in how the thickness of the IMH edges changed across the study groups. Baseline HEI-t values were 378.10±15.47 μm in Group 1, 373.13±15.69 μm in Group 2, and 373.96±15.08 μm in Group 3. One month after surgical treatment, the value in Group 1 decreased to 259.61±12.96 μm. In contrast, Group 2 showed an increase to 391.94±16.14 μm, while the HEI-t value in Group 3 was 358.53±15.00 μm. However, later, HEI-t value decreased in all groups: e.g., by 12 months, the values were 230.03±5.82 μm, 343.29±12.02 μm, and 296.5±14.6 μm, respectively. The most pronounced reduction in HEI-t value was observed in Group 1 patients.

A similar pattern was observed for the HEI-n metric. Prior to surgical treatment, its values were 381.42±17.60 μm in Group 1, 387.29±12.26 μm in Group 2, and 380.27±18.54 μm in Group 3. After 12 months, these values decreased to 237.30±6.28 μm, 353.29±9.75 μm, and 283.00±18.8 μm, respectively. Therefore, in Group 1, the reduction in both HEI-t and HEI-n values was more pronounced than in the other groups (*Table* 2).

As for the MRTOE-t metric, its baseline values were 261.00±7.54 μm in Group 1, 264.13±7.20 μm in Group 2, and 266.85±7.57 μm in Group 3. One month after surgical treatment, we observed an increase in this parameter up to 280.19±8.49, 280.81±8.28, and 281.15±7.64 μm, respectively. Later on, by the sixth month, MRTOE-t values declined to 274.12±7.99, 275.13±8.07, and 276.89±7.92 μm, respectively. While the mean values of epш metric remained similar across the groups, an analysis of the trends revealed a statistically significant *time* × *group* interaction ($p<0.001$), thereby indicating differences in the pattern of MRTOE-t changes during the postoperative period (*Table* 3).

In the postoperative period, the proposed FCI and FSCI morphometric indices exhibited progressive changes, reflecting the extent of autograft contraction (*Figures* 2*a* and 2*b*) and the remodeling of the donor site (*Figures* 2*c* and 2*d*), respectively.

Unlike conventional morphometric parameters, which characterize individual anatomical structures, these indices provide the quantitative assessment of the structural integration of an autograft. A progressive decrease in FCI values indicate the formation of a tighter contact between the autograft and the surrounding retina, while a reduction in FSCI values reflect the completion of repair processes in the donor site and the stabilization of its microarchitecture (*Table* 4).

Based on an analysis of the dynamics of these morphometric parameters, we identified three successive phases of repair: the early adaptation phase, the structural integration phase, and the morphological remodeling phase. Each phase was characterized by specific changes in the morphometric parameters, reflecting the status of the autograft, the surrounding retina, and the donor site (*Figure* 3).

The early adaptation phase corresponds to the first month after surgical treatment. During this period, we observed a reduction in the HEI values (this metric characterizes the height of the macular hole edges), along with changes in parameters related to the positioning and contraction of the graft.

The structural integration phase covers the period up to three months after surgery and is characterized by a further decline in the HEI value and changes in the FCI value, thereby reflecting the structural reorganization of the graft within the IMH area. Concurrently, we noted a trend toward stabilization of the MRTOE metric.

Table 2. Quantitative dynamics of the macular hole edge elevation indices of the temporal (HEI-t) and nasal (HEI-n) edges in the study groups

Parameter	Group	Treatment duration				
		Before intervention	After surgery, months			
			1	3	6	12
HEI-t	1	378.1±15.47; 381 [372; 390]	259.61±12.96; 261 [248; 267]	247.39±11.06; 249 [236; 256]	236.55±9.81; 239 [227; 244]	230.03±5.82; 232 [223; 234]
	2	373.13±15.69; 373 [363; 381]	391.94±16.14; 392 [382; 401]	375.19±14.45; 377 [370; 385]	356.45±14.84; 355 [350; 364]	343.29±12.02; 345 [335; 353]
	3	373.96±15.08; 374 [362; 384]	358.53±15.00; 359 [347; 370]	339.33±15.51; 339 [327; 353]	298.95±15.96; 300 [287; 310]	296.5±14.6; 300 [287; 310]
HEI-n	1	381.42±17.60; 379 [369; 389]	269.70±15.57; 263 [259; 281]	256.36±12.37; 253 [247; 269]	245.06±9.71; 244 [239; 252]	237.30±6.28; 240 [231; 241]
	2	387.29±12.26; 385 [380; 399]	401.46±11.79; 403 [393; 412]	387.77±10.00; 390 [383; 394]	372.94±10.81; 373 [368; 382]	353.29±9.75; 353 [347; 360]
	3	380.27±18.54; 380 [366; 392]	364.89±18.33; 363 [351; 377]	345.59±19.43; 346 [332; 357]	293.00±19.36; 293 [282; 302]	283.00±18.8;293 [282; 302]

Table 3. Quantitative dynamics of the retinal thickness measurements outside the edematous zone represented by the mean reference thickness over edema indices of the temporal edge (MRTOE-t) and nasal edge (MRTOE-n) of the macular region in the study groups

Parameter	Group	Treatment duration				
		Before intervention	After surgery, months			
			1	3	6	12
MRTOE-t	1	261.00±7.54; 261 [255; 266]	280.19±8.49; 280 [272; 288]	277.58±8.62; 276 [271; 285]	274.12±7.99; 274 [267; 281]	272.2±7.81; 274 [267; 281]
	2	264.13±7.20; 263 [258; 270]	280.81±8.28; 281 [275; 288]	278.13±8.23; 279 [272; 285]	275.13±8.07; 275 [270; 281]	273.1±8.07; 275 [270; 280]
	3	266.85±7.57; 268 [260; 273]	281.15±7.64; 282 [275; 287]	277.02±7.55; 277 [271; 284]	276.89±7.92; 278 [271; 284]	275.9±7.89; 278 [269; 283]
MRTOE-n	1	262.31±7.52; 262 [257; 269]	282.06±7.62; 280 [276; 288]	279.45±7.70; 278 [274; 284]	276.39±7.50; 274 [270; 283]	274.3±7.41; 274 [270; 279]
	2	260.88±7.34; 260 [255; 267]	283.26±7.01; 284 [278; 289]	280.68±7.16; 282 [276; 287]	277.74±7.19; 278 [271; 283]	276.3±7.19; 278 [270; 281]
	3	261.26±7.54; 260 [255; 269]	282.54±7.45; 281 [277; 289]	278.56±7.58; 278 [274; 284]	277.63±8.16; 278 [271; 282]	275.3±8.2; 278 [271; 282]

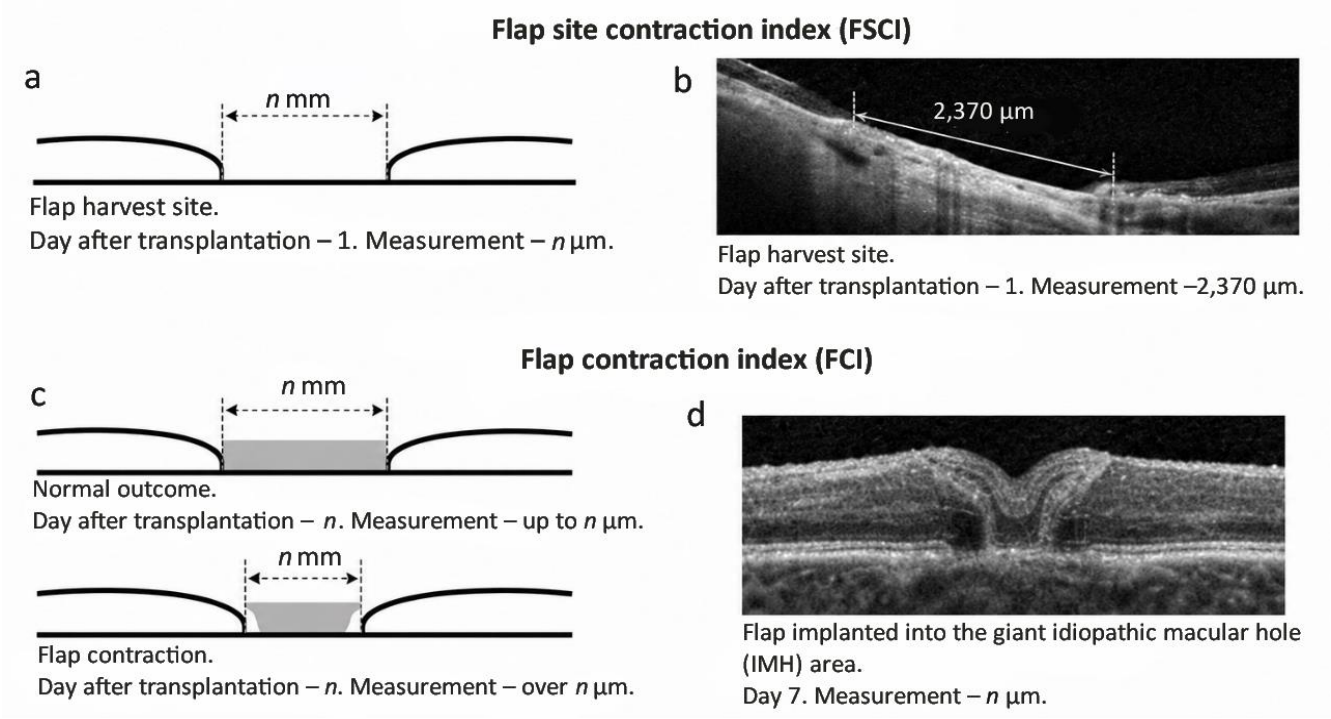

Figure 2. Contraction index values for the autograft and the donor site.

© Stepanenko A.I., Fayzrakhmanov R.R., Konovalova K.I., Borodkina V.N., 2026

Table 4. Quantitative dynamics of the contraction indices for the autograft (flap contraction index [FCI]) and the donor site (flap site contraction index [FSCI]) in the study groups

Group	After surgery, months			
	1	3	6	12
FCI				
1	1672.76±179.01; 1653 [1537; 1739]	1550.73±180.81; 1521 [1411; 1641]	1463.55±183.52; 1435 [1331; 1536]	1463.55±183.52; 1435 [1331; 1536]
2	1734.87±127.03; 1730 [1622; 1806]	1612.74±127.63; 1610 [1492; 1691]	1524.45±132.91; 1516 [1431; 1594]	1524.45±132.91; 1516 [1431; 1594]
FSCI				
1	1495.21±200.71; 1472 [1333; 1589]	1495.21±200.71; 1472 [1333; 1589]	1368±202.2; 1354 [1217; 1438]	1144.64±202.96; 1133 [1004; 1223]
2	1548.1±133.56; 1535 [1448; 1634]	1548.1±133.56; 1535 [1448; 1634]	1414.26±126.96; 1401 [1311; 1520]	1196.45±138.22; 1187 [1094; 1278]

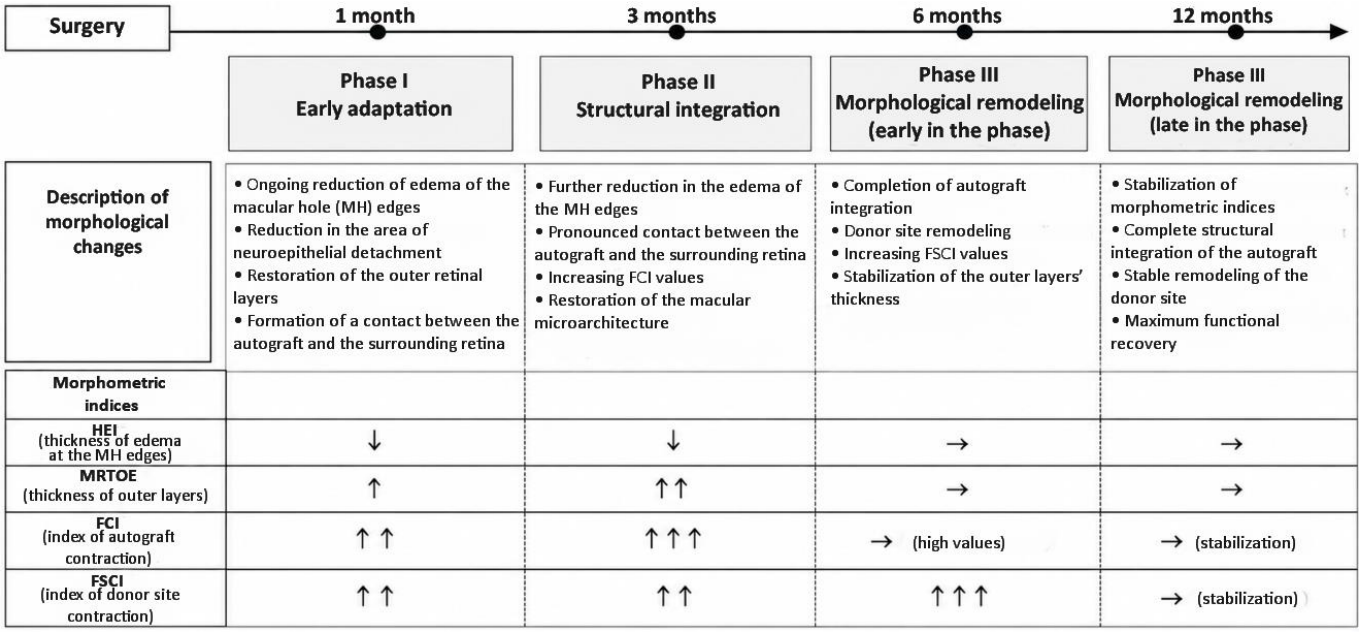

Figure 3. Morphometric model of repair following autologous neurosensory retinal transplantation for giant idiopathic macular holes.

Between 6 and 12 months after surgery, changes corresponding to the morphological remodeling phase became predominant. During this timeframe, several morphometric parameters stabilized, while the FSCI (which reflects changes in the donor site) continued to demonstrate dynamic changes.

Discussion

The results of our study indicate that the repair processes after ART for giant IMHs are characterized by a consistent sequence of morphological changes. These reflect the structural adaptation of the graft, its integration with the surrounding tissues, and the subsequent remodeling of the donor site [6, 10]. Unlike many published studies, which primarily focused on the anatomical closure rate of the IMH and changes in BCVA, our study provides a comprehensive quantitative assessment of postoperative changes based on a set of OCT-derived morphometric parameters [5].

Our findings are consistent with those of D.S. Grewal et al., who demonstrated in a multicenter study that ART is highly effective for treating refractory and large macular holes. They observed the restoration of the external limiting membrane and the ellipsoid zone on OCT, alongside an improvement of visual functions [3]. Yet their study focused mainly on anatomical and functional outcomes rather than a sequential analysis of structural repair processes using a comprehensive set of morphometric parameters.

Our data also comply with the results of a study by H. Tabandeh, who used multimodal imaging (including OCT, OCT angiography, and fluorescein angiography) to demonstrate the processes of vascularization, reperfusion, and early structural integration of the autograft during the postoperative period. Tabandeh attributed functional recovery to the gradual adaptation of the graft and its interaction with the surrounding retina. However, the aforementioned study did not include a comprehensive quantitative assessment of the successive phases of repair using a system of morphometric indices [11].

A key distinction of the present study is the development of a morphometric model of repair, based on a comprehensive assessment of the dynamics of the HEI, MRTOE, FCI, and FSCI indices, which made it possible to identify the successive phases of postoperative repair (early adaptation, structural integration, and morphological remodeling) and to characterize the specific features of these processes under various surgical treatment approaches. This method provides an opportunity for a transition from analyzing individual morphological features to a comprehensive assessment of the structural recovery processes in the macular region.

It should be noted that the most favorable dynamics of the morphometric parameters was observed in patients who

underwent edge-to-edge ART. This ART technique was associated with a more pronounced decrease in the HEI value, lower variability in the MRTOE, and an earlier stabilization of the FCI and FSCI values. These combined findings may indicate a better progression of the processes involving the structural integration of the autograft and the remodeling of the donor site.

The proposed morphometric model of reparative changes can serve as an additional tool for the objective assessment of postoperative dynamics in patients after ART.

Conclusion

Repair processes following ART for giant IMHs are characterized by a successive progression of morphometric parameters, as assessed via OCT. A comprehensive evaluation of the HEI, MRTOE, FCI, and FSCI metrics allows for an objective assessment of the structural adaptation and integration of the graft, as well as the remodeling processes occurring in the donor site. The proposed morphometric model systematizes the key phases of retinal structural recovery after ART and enhances the objective interpretation of OCT data. The application of this set of morphometric parameters can serve as an additional tool for evaluating postoperative progress and comparing the efficacy of various ART techniques for giant IMHs.

Conflict of interest

None declared by the authors.

Author contributions

All authors contributed equally to the preparation of this manuscript.

Informed consent for publication

All patients signed a voluntary informed consent form for the publication of their medical information.

Funding

The authors declare no external funding for the conduct of the research or the publication of this article.

Compliance with ethical principles

The study protocol was approved by the local ethics committee. The approval and the implementation of the protocol were in accordance with the principles of the Declaration of Helsinki.

References

1. Arda H, Maier M, Schultheiß M, Haritoglou C. Advances in management strategies for large and persistent macular hole: An update. *Surv Ophthalmol* 2024; 69(4): 539-546. https://doi.org/10.1016/j.survophthal.2024.03.010.
2. Zhang R, Fang YC, Shi X, et al. Meta-regression of idiopathic full-thickness macular holes diameter and anatomical closure rate: Implications to intraoperative technique. *Heliyon* 2024; 10(17): e36588. https://doi.org/10.1016/j.heliyon.2024.e36588.
3. Grewal DS, Charles S, Parolini B, et al. Autologous retinal transplant for refractory macular holes: Multicenter International Collaborative Study Group. *Ophthalmology* 2019; 126(10): 1399-1408. https://doi.org/10.1016/j.ophtha.2019.01.027.
4. Moysidis SN, Koulisis N, Adrean SD, et al. Autologous retinal transplantation for primary and refractory macular holes and macular hole retinal detachments: The Global Consortium. *Ophthalmology* 2021; 128(5): 672-685. https://doi.org/10.1016/j.ophtha.2020.10.007.
5. Hanai M, Amaral DC, Jacometti R, et al. Large macular hole and autologous retinal transplantation: A systematic review and meta-analysis. *Int J Retina Vitreous* 2024; 10(1): 56. https://doi.org/10.1186/s40942-024-00573-1.
6. Rojas-Juárez S, Cisneros-Cortés J, Ramirez-Estudillo A, Velez-Montoya R. Autologous full-thickness retinal transplant for refractory large macular holes. *Int J Retina Vitreous* 2020; 6(1): 60. https://doi.org/10.1186/s40942-020-00266-5.
7. Hernández-Da Mota SE, Morales-Cantón V, Rojas-Juárez S, et al. Autologous retinal transplant for macular hole. *Open Ophthalmol J* 2021; 15: 292-298. https://doi.org/10.2174/1874364102115010292.
8. Yu Y, Liang X, Wang Z, et al. Clinical and morphological comparisons of idiopathic macular holes between phase 3 and phase 4. *Graefes Arch Clin Exp Ophthalmol* 2018; 256(12): 2327-2333. https://doi.org/10.1007/s00417-018-4158-7.
9. Kitahata S, Inoue T, Nagura K, et al. Retinal morphologic features in patients with large macular holes treated by autologous neurosensory retinal transplantation. *Ophthalmol Retina* 2023; 7(5): 406-412. https://doi.org/10.1016/j.oret.2022.12.004.
10. Lumi X, Petrovic Pajic S, Sustar M, et al. Autologous neurosensory free-flap retinal transplantation for refractory chronic macular hole – Outcomes evaluated by OCT, microperimetry, and multifocal electroretinography. *Graefes Arch Clin Exp Ophthalmol* 2021; 259(6): 1443-1453. https://doi.org/10.1007/s00417-020-04981-5.
11. Tabandeh H. Vascularization and reperfusion of autologous retinal transplant for giant macular holes. *JAMA Ophthalmol* 2020; 138(3): 305-309. https://doi.org/10.1001/jamaophthalmol.2019.5733.

Authors:
Anastasia I. Stepanenko – Graduate Student, Department of Eye Diseases, Institute for Advanced Medical Training, Pirogov National Medical and Surgical Center, Moscow, Russia. https://orcid.org/0000-0002-7979-3490;
Rinat R. Fayzrakhmanov – DSc (Medicine), Professor, Chair of the Department of Ophthalmology, Institute for Advanced Medical Training; Head of the Center for Ophthalmology, Pirogov National Medical and Surgical Center, Moscow, Russia. https://orcid.org/0000-0002-4341-3572;
Karina I. Konovalova – PhD (Medicine), Assistant Professor, Department of Ophthalmology, Institute for Advanced Medical Training; Ophthalmologist, Center for Ophthalmology, Pirogov National Medical and Surgical Center, Moscow, Russia. https://orcid.org/0000-0002-5517-9111;
Vera N. Borodkina – Resident, Department of Eye Diseases, Institute for Advanced Medical Training, Pirogov National Medical and Surgical Center, Moscow, Russia.